



ORIGINAL RESEARCH COMMUNICATION

Alterations in Mitochondrial Function in Pulmonary Vascular Diseases

Samar Farha,^{1,2} Kewal Asosingh,¹ Paul M. Hassoun,³ John Barnard,¹ Suzy Comhair,¹ Andrew Reichard,¹ Nicholas Wanner,¹ Milena Radeva,¹ Micheala A. Aldred,⁴ Gerald J. Beck,¹ Erika Berman-Rosenzweig,⁵ Barry A. Borlaug,⁶ J. Emanuel Finet,⁷ Robert P. Frantz,⁶ Gabriele Grunig,⁸ Anna R. Hemnes,⁹ Nicholas Hill,¹⁰ Evelyn M. Horn,¹¹ Christine Jellis,⁷ Jane A. Leopold,¹² Reena Mehra,¹³ Margaret M. Park,⁷ Franz P. Rischard,¹⁴ W.H. Wilson Tang,^{1,7} and Serpil C. Erzurum^{1,2}; the PVDOMICS Study Group

Abstract

Aims: Alterations of mitochondrial bioenergetics and arginine metabolism are universally present and mechanistically linked to pulmonary arterial hypertension (PAH), but there is little knowledge of arginine metabolism and mitochondrial functions across the different pulmonary hypertension (PH) groups. We hypothesize that abnormalities in mitochondrial functions are present across all PH groups and associated with clinical phenotypes. We test the hypothesis in PH patients and healthy controls from the Pulmonary Vascular Disease Phenomics Program cohort, who had comprehensive clinical phenotyping and follow-up for at least 4 years for death or transplant status. Mitochondrial transmembrane potential, superoxide production, and mass were measured by flow cytometry in fresh platelets. Metabolomics analysis was performed on plasma samples. Global arginine bioavailability was calculated as the ratio of arginine/(ornithine+citrulline).

Results: Global arginine bioavailability is consistently lower than controls in all PH groups. Although the mitochondrial mass is similar across all PH groups and controls, superoxide production and transmembrane potential vary across groups. Mitochondrial superoxide is higher in group 1 PAH and lowest in group 3 compared with other groups, while transmembrane potential is lower in group 1 PAH than controls or group 3. The alterations in mitochondrial functions of group 1 PAH are associated with changes in fatty acid metabolism. Mitochondrial transmembrane potential in group 1 PAH is associated with transplant-free survival.

Conclusion: While alterations in mitochondrial function are found in all PH groups, group 1 PAH has a unique mitochondrial phenotype with greater superoxide and lower transmembrane potential linked to fatty acid metabolism, and clinically to survival. *Antioxid. Redox Signal.* 42, 361–377.

¹Integrated Hospital-Care Institute, Cleveland Clinic, Cleveland, Ohio, USA.

²Lerner Research Institute, Cleveland Clinic, Ohio, USA.

³Division of Pulmonary and Critical Care Medicine, Johns Hopkins Hospital, Baltimore, Maryland, USA.

⁴Department of Medicine, Indiana University School of Medicine Indianapolis, Indianapolis, Indiana, USA.

⁵Department of Pediatrics and Medicine, Columbia University, New York, New York, USA.

⁶Department of Cardiovascular Medicine, Mayo Clinic, Rochester, Minnesota, USA.

⁷Heart Vascular and Thoracic Institute, Cleveland Clinic, Cleveland, Ohio, USA.

⁸Department of Environmental Medicine, New York University Grossman School of Medicine, New York, New York, USA.

⁹Division of Allergy, Pulmonary and Critical Care Medicine, Vanderbilt University Medical Center, Nashville, Tennessee, USA.

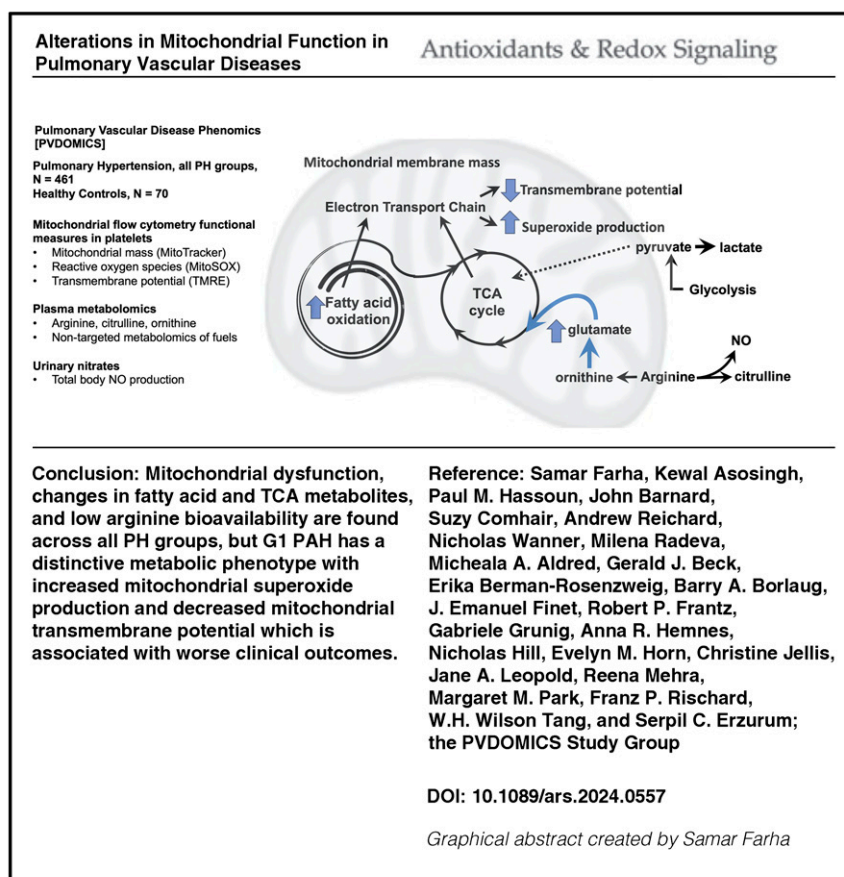
¹⁰Division of Pulmonary, Critical Care, and Sleep Medicine, Tufts Medical Center, Boston, Massachusetts, USA.

¹¹Division of Cardiology, Weill Cornell Medical Center, New York, New York, USA.

¹²Division of Cardiovascular Medicine, Brigham and Women's Hospital, Harvard Medical School., Boston, Massachusetts, USA.

¹³Division of Pulmonary, Critical Care and Sleep Medicine, University of Washington, Seattle, Washington, USA.

¹⁴Division of Pulmonary, Allergy, Critical Care and Sleep Medicine, University of Arizona, Tucson, Arizona, USA.



Keywords: pulmonary hypertension, mitochondria, arginine metabolism, transmembrane potential, superoxide production

Introduction

Pulmonary arterial hypertension (PAH) is a progressive and often lethal disorder disproportionately afflicting women and is a subclass of a broader group of pulmonary vascular diseases. Pulmonary vascular diseases are classified by clinical conditions associated with pulmonary hypertension (PH) based on similar pathophysiological mechanisms, clinical presentation, hemodynamics, and therapeutic management into five groups. Group 1 (G1) PAH includes idiopathic, heritable, drug- and toxin-induced, associated forms,

PAH with features of venous/capillary involvement, and persistent PH of the newborn. G2 PH is secondary to the left heart diseases, G3 is associated with lung diseases or hypoxia, G4 is due to chronic pulmonary artery obstruction, and G5 includes diseases with multifactorial or unclear mechanisms (Humbert et al., 2022; Simonneau et al., 2013).

Multiple lines of evidence from preclinical models, human cells derived from PAH lungs, and studies of patients identify abnormalities of metabolic pathways in the molecular pathogenesis of PAH, including abnormalities in mitochondrial numbers, mitochondrial oxidative phosphorylation, decreased electron transport chain (ETC) function in vascular cells from PAH lungs, and shift to greater glycolysis and glucose uptake in hearts, lungs, and skeletal muscles in PAH patients (Bonnet et al., 2006; Egnatchik et al., 2017; Malenfant et al., 2015; Pak et al., 2013; Xu et al., 2021; Xu et al., 2007). In parallel to bioenergetic changes, PAH is mechanistically linked to abnormalities of arginine metabolism. Arginine is the substrate for endothelial nitric oxide (NO) synthase, which converts arginine to NO and citrulline. Loss of NO production in PAH is associated with greater mitochondrial arginine metabolism *via* arginase, which converts arginine to ornithine (Ghosh et al., 2016; Kaneko et al., 1998; Klinger et al., 2013; Machado et al., 2004; Ozkan et al., 2001; Tonelli et al., 2013; Xu et al., 2004; Xu et al., 2007). Thus, alterations

Innovation

There is a need to expand our understanding of metabolic abnormalities and mitochondrial dysfunction across the spectrum of pulmonary vascular diseases. This is the first study measuring mitochondrial function and arginine bioavailability in a large cohort of well-phenotyped patients with PH and across all five groups in comparison with healthy controls. Our findings highlight the decreased arginine bioavailability across all PH groups and heterogeneity in platelet mitochondrial function among the different groups, and reveal shifts in fuel use that link to disease types and severity.

of arginine/NO metabolism are biochemically linked to abnormalities of mitochondrial bioenergetics (Nisoli and Caruba, 2006).

With early reports of metabolic interventions for the treatment of PH showing encouraging results (Archer et al., 2010; Fang et al., 2012; Farha et al., 2017; Michelakis et al., 2017; Paddenberg et al., 2007; Piao et al., 2013; Piao et al., 2010; Seyfarth et al., 2013; Sharma et al., 2013; Sharp et al., 2014), targeting mitochondrial pathways offers a promising approach to developing new therapeutic options. However, in multifactorial diseases such as PH, mitochondrial function may vary from patient to patient, and over time, and may be affected by various factors, including therapies, underscoring the need for a precision approach in applying metabolic interventions. There is a need to quantify mitochondrial function, a task limited by the lack of ready availability of mitochondria from affected tissues. Recent work suggests that platelets can serve as a valid measure of mitochondrial function in diseases (Ben-Shachar et al., 2007; Guo et al., 2009; Parker et al., 1990a, 1990b; Parker et al., 1989; Rezanian et al., 2017; Sangiorgi et al., 1994; Shi et al., 2008; Zharikov and Shiva, 2013). Platelets may be a particularly important site to study mitochondria in PAH. *In situ* thrombosis and abnormal platelet aggregation are hallmarks of PAH, and platelets have been implicated in PAH pathogenesis through the release of proinflammatory, angiogenic, and prothrombotic mediators (Aytekin et al., 2012; Herve et al., 2001; Lannan et al., 2014).

Despite substantial knowledge on alterations in mitochondrial bioenergetics and arginine–NO metabolism in G1 PAH, there is still a need to quantify mitochondrial function, which is limited by access to mitochondria from affected tissues. Furthermore, there is a gap in our understanding of these pathways in other PH groups. In this study, we hypothesize that (1) abnormalities in mitochondrial function are present in PH and are associated with clinical groups and/or phenotypes and (2) platelets can be used to assess the metabolic shift and mitochondrial dysfunction of the pulmonary vascular bed. We explore metabolic pathways associated with mitochondrial activity to uncover mechanistic connections between mitochondrial function and PH. The findings are summarized in the Graphical Abstract.

Results

Study population

The study population of the Pulmonary Vascular Disease Phenomics (PVDOMICS) cohort has been previously described (Hemnes et al., 2022). The subgroup for this analysis consists of 70 healthy controls and 461 patients with PH. Demographics are outlined in Table 1. While there is no difference in race distribution, there is a significant difference in age and sex distribution between healthy controls and PH participants. Healthy controls are younger and have a higher proportion of women compared with PH participants (Table 1).

Effect of sex, race, and age on mitochondrial mass and function

Sex, race differences, and aging-related changes in mitochondrial biogenesis and bioenergetics are described in health and disease states. We thus explored the effect of sex, age, and race in our cohort and found that the mitochondrial

mass is higher in Black participants ($p = 0.008$) and inversely related to age ($R = -0.1$, $p = 0.03$) (Fig. 1). Mitochondrial transmembrane potential and superoxide production do not correlate with race and age. Moreover, mitochondrial mass and superoxide production are not affected by sex. Transmembrane potential tends to be lower in women ($p = 0.06$) (Fig. 1). All analyses of mitochondrial assays are thus adjusted for age, sex, and race. Among mitochondrial measures, the mitochondrial mass correlates weakly with mitochondrial superoxide production ($R = 0.15$, $p < 0.001$). There is no correlation between mitochondrial mass and transmembrane potential in the study cohort ($p = 0.2$). On the contrary, transmembrane potential is inversely related to superoxide production ($R = -0.25$, $p < 0.001$) (Fig. 2).

Alterations in mitochondrial transmembrane potential and superoxide production

There are no significant differences in mitochondrial mass or function between healthy controls and all patients with PH (all $p > 0.1$). While mitochondrial mass does not differ by PH groups, mitochondrial function is significantly different across the PH groups. G3 PH has the lowest superoxide production, significantly lower than G1 and G2 PH. G1 PAH tends to have a lower mitochondrial transmembrane potential compared with healthy controls and G2 PH and significantly lower transmembrane potential compared with G3 PH (Table 2) (Fig. 3).

PH therapies and management vary based on PH groups with most PH-specific therapies used in G1 PAH and G4 PH. In the PH cohort, 82% of G1 PAH patients are on PH therapies compared with 24% of G2 PH, 35% of G3 PH, 37% of G4 PH, and 53% of G5 PH patients. Mitochondrial transmembrane potential is lower in patients on PH therapies ($p < 0.001$), whereas superoxide production is not different between the two groups ($p = 0.5$). Likewise, when comparing prevalent cases with incident cases, mitochondrial transmembrane potential is lower and superoxide production higher in prevalent cases compared with incident (both $p < 0.01$). Mitochondrial transmembrane potential is inversely associated with years since PH diagnosis ($R = -0.15$, $p = 0.002$). Propensity score analysis using sex, age, race, and PH medications as confounders reveals a significant difference in transmembrane potential and superoxide production among all PH groups (both $p \leq 0.01$). Superoxide production is significantly higher in G1 compared with G3 PH using Bonferroni-adjusted significance level <0.005 for pairwise comparison (Supplementary Table S1).

Another important clinical aspect to PH grouping is that patients often have a mixed etiology of their disease, that is, they fit more than one of the current PH classification groups. In this cohort, 39% have overlap of PH classification (Hemnes et al., 2022). To adjust for overlap in classifications, analyses are also performed with exclusion of patients with mixed groups ($N = 183$). The differences in mitochondrial transmembrane potential and higher superoxide production between G1 and G3 PH remain statistically significant (both $p < 0.001$) after excluding patients with mixed PH etiologies.

Arginine–NO pathway

Arginine–NO pathway abnormalities are well described in preclinical models of PH and in G1 PAH, and abnormalities

TABLE 1. DEMOGRAPHICS OF STUDY COHORT

	<i>Controls</i>	<i>PH</i>	<i>p Value</i>
	N = 70	N = 461	
Age (years)	47 ± 14	59 ± 15	<0.001
Race, <i>n</i> (%)			0.2
Caucasian	59 (84%)	354 (77%)	
African American	9 (13%)	65 (14%)	
Others	2 (3%)	42 (9%)	
Sex, <i>n</i> (%)			0.05
Female	52 (74%)	286 (62%)	
Male	18 (26%)	175 (38%)	
Pulmonary hypertension groups, <i>n</i> (%)			
Group 1		202 (44%)	
Group 2		90 (19%)	
Group 3		109 (24%)	
Group 4		41 (9%)	
Group 5		19 (4%)	
PAH-specific therapies, <i>n</i> (%)			
Phosphodiesterase type 5 inhibitors/stimulator of soluble guanylate cyclase		209 (45%)	
Endothelin receptor antagonist		134 (29%)	
Prostacyclin/prostacyclin receptor agonist		95 (21%)	
Temperature (Fahrenheit)	98.0 ± 0.6	97.9 ± 0.6	0.1
Pulse (beats/min)	71 ± 11	77 ± 14	<0.001
O ₂ saturation (%)		94 ± 4	<0.001
RVSP (mmHg)	24 ± 5	60 ± 23	<0.001
Hemodynamic variables			
Right atrial pressure (mmHg)		7 [4, 11]	
Mean pulmonary arterial pressure (mmHg)		38 [30, 49]	
Pulmonary capillary wedge pressure (mmHg)		12 [8, 16]	
Cardiac output (l/min)		5.2 ± 1.8	
Pulmonary vascular resistance (Wood units)		4.8 [3.1, 7.7]	
6-Minute walk distance (m)	529 ± 101	337 ± 140	<0.001
NT-proBNP (pg/mL)	48 [23, 74]	331 [112, 1423]	<0.001
WHO functional class (I/II/III/IV)		33/150/235/25	

Statistics presented as mean ± SD, median [P25, P75], N (column %).

PH, pulmonary hypertension; PAH, pulmonary arterial hypertension; O₂, oxygen; RVSP, right ventricular systolic pressure; NT-proBNP, N-terminal pro-brain natriuretic protein; WHO, World Health Organization.

are associated with abnormal bioenergetics (Afolayan et al., 2016; Aytekin et al., 2012; Farha et al., 2021; Ghosh et al., 2016; Kao et al., 2015; Xu et al., 2004), but little is known about this pathway in other PH groups. Targeted metabolomics of arginine pathway metabolites across PH groups and controls shows that arginine is not different among PH and controls (arginine [μ M]: controls 104.3 [88.3, 123.6], PH 98.4 [80.9, 120.7]; $p = 0.2$). However, citrulline and ornithine levels are significantly higher in PH compared with controls (citrulline [μ M]: controls 34.5 [27.1, 42.7], PH 39.7 [32.3, 51.2]; $p < 0.001$ and ornithine [μ M]: controls 66.8 [55.8, 81.7], PH 75.7 [59.0, 93.0]; $p = 0.02$). Thus, similar to prior reports of G1 PAH (Kao et al., 2015; Morris et al., 2005; Simpson et al., 2023; Xu et al., 2021), the global arginine bioavailability ratio (GABR) is significantly lower in PH compared with controls (GABR: controls 1.08 [0.9, 1.3], PH 0.88 [0.69, 1.10]; $p < 0.001$). There is no significant difference between the groups in urinary nitrate, a stable salt of NO excreted in urine ($p = 0.1$) (Xu et al., 2007).

Arginine is also not different among the various PH groups ($p = 0.5$). Citrulline and ornithine vary significantly among groups with higher levels in G2 PH (Table 2). GABR varies

among PH groups with lower levels in G2 PH (Table 2). Results remain significant after using propensity score to adjust for PH medication use (Supplementary Table S1). Urinary nitrate is higher in G1 PAH compared with G2 PH (Table 2); however, this is not significant after adjusting for PH medications using propensity score analysis. These analyses show a previously unknown heterogeneity of the arginine-NO pathway among PH groups, and provide insight to the pathophysiology of the different cardiovascular phenotypes.

Mitochondrial function and bioenergetics: the tricarboxylic acid cycle

Both tricarboxylic acid (TCA) cycle and fatty acid β -oxidation use fuels in reactions to provide Nicotinamide Adenine Dinucleotide (NADH) and Flavin Adenine Dinucleotide (FADH₂) for the ETC in the inner mitochondrial membrane to pump protons and generate a transmembrane potential that is used to produce energy, heat, and reactive oxygen species (ROS). In this study, abnormalities of metabolism are related to mitochondrial transmembrane potential and superoxide production using nontargeted metabolomic data. The differences in TCA metabolites among PH groups and controls are

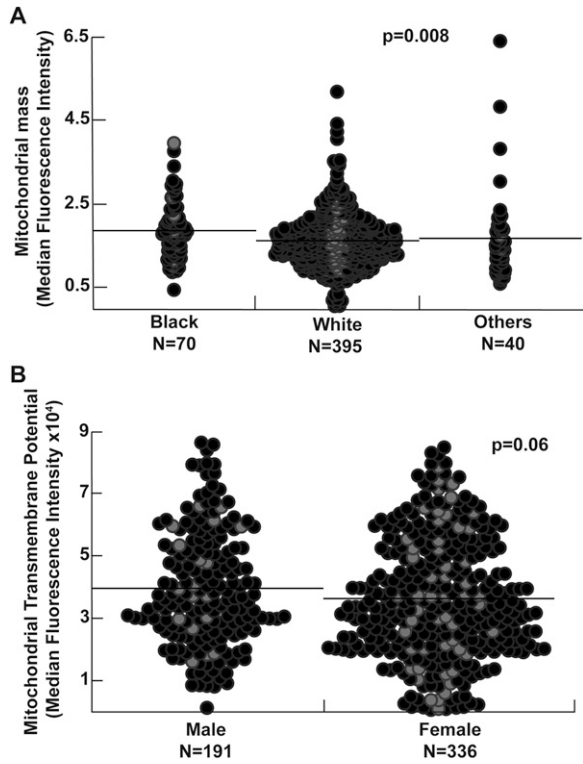


FIG. 1. Effect of sex and race on mitochondrial assays. (A) Mitochondrial mass was significantly higher in Black participants. Mitochondrial transmembrane potential and superoxide production were not affected by race. (B) Male participants tended to have higher mitochondrial transmembrane potential. Mass and superoxide production were not affected by sex. Individual data points shown. Black line represents the mean. Gray circles represent controls, and black circles pulmonary hypertension (PH). Wilcoxon *p* value used.

shown in Figure 4 and Table 3. TCA metabolites dependent on mitochondrial complex 1 NADH dehydrogenase activity differ across PH groups and controls (Fig. 4). There is a

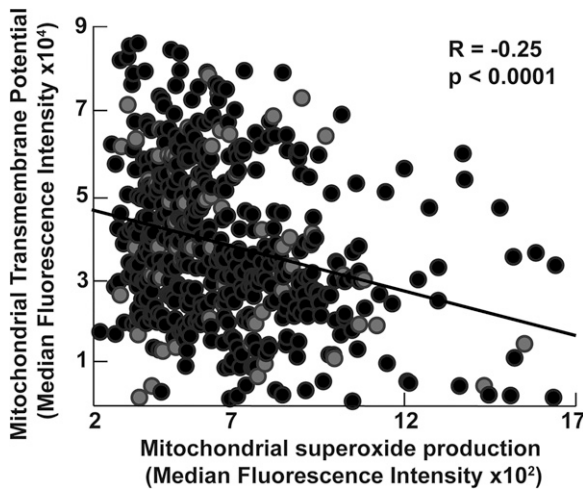


FIG. 2. Mitochondrial transmembrane potential is inversely related to superoxide production. In our overall cohort, there is an inverse correlation between mitochondrial transmembrane potential and superoxide production. Pearson's correlation used with line of best fit shown for visualization.

TABLE 2. MITOCHONDRIAL ASSAYS AND ARGININE PATHWAY (TARGETED) METABOLITES ACROSS PULMONARY HYPERTENSION GROUPS AND CONTROLS

	Controls	G1 PH	G2 PH	G3 PH	G4 PH	G5 PH	<i>p</i> Value
Mitochondrial mass (MFI)	1.6 [1.2, 1.9]	1.6 [1.3, 1.9]	1.6 [1.3, 1.9]	1.5 [1.2, 1.9]	1.7 [1.3, 2.0]	1.8 [1.3, 2.2]	0.9
Mitochondrial superoxide production (MFI × 10 ²)	6.3 [5.0, 8.0]	6.6* [5.3, 8.5]	6.2 [5.4, 8.2]	5.7* [4.7, 7.2]	6.9 [5.3, 8.0]	5.8 [4.5, 8.4]	0.01
Mitochondrial transmembrane potential (MFI × 10 ⁴)	3.7 [2.1, 5.6]	3.2* [2.2, 4.4]	3.6 [2.6, 5.5]	4.2* [2.9, 5.8]	3.3 [2.8, 4.8]	2.7 [1.9, 5.2]	0.007
Arginine (μM)	104.1 [88.3, 123.6]	99.6 [82.0, 120.6]	94.3 [81.2, 116.1]	98.7 [77.7, 124.0]	109.5 [87.8, 125.8]	106.2 [73.5, 129.7]	0.4
Ornithine (μM)	66.8 [55.8, 81.7]	73.6* [54.9, 89.0]	85.8*† [70.5, 145.6]	71.8† [60.5, 88.2]	76.5 [63.1, 90.5]	77.3 [58.9, 82.4]	0.04
Citrulline (μM)	34.5 [27.1, 42.7]	39.1* [32.2, 47.5]	49.4*† [36.3, 65.0]	37.6† [30.5, 46.8]	41.1† [34.2, 52.2]	40.0 [31.5, 57.9]	<0.001
GABR	1.08 [0.91, 1.26]	0.94* [0.73, 1.14]	0.76*† [0.54, 0.93]	0.88*† [0.71, 1.11]	0.85† [0.67, 1.14]	0.92 [0.73, 1.13]	0.009
Urinary nitrate/creatinine (μmol/μmol)	0.07 [0.04, 0.09]	0.07* [0.04, 0.09]	0.04* [0.03, 0.08]	0.06 [0.04, 0.09]	0.05 [0.03, 0.07]	0.04 [0.03, 0.08]	0.4

Statistics presented as median [P25, P75], Kruskal–Wallis *p* value adjusted for age, sex, and race. Significant pairwise analyses between PH groups are marked with *, †. PH groups that are significantly different from controls are marked with #. Bonferroni-adjusted significance level <0.003 for multiple comparisons. GABR, global arginine bioavailability ratio; MFI, mean fluorescence intensity.

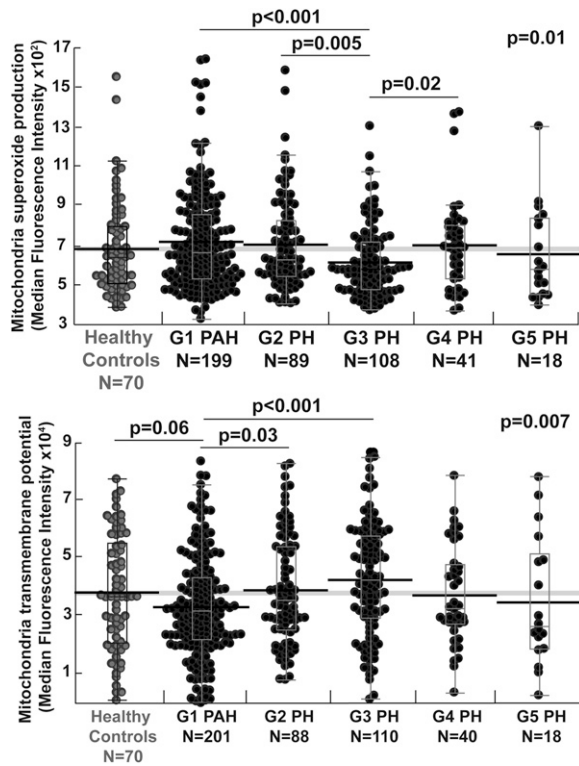


FIG. 3. Group1 (G1) pulmonary arterial hypertension (PAH) has lower mitochondrial transmembrane potential and higher superoxide production. Mitochondrial transmembrane potential and superoxide production varied across PH groups. G1 PAH had significantly lower transmembrane potential compared with G2 and 3 PH and a tendency for lower transmembrane potential compared with healthy controls. G3 PH had lower superoxide production compared with G1, 2, and 4 PH. Gray circles represent controls and black circles PH. Box plots show median and 25%–75% quartiles. Whiskers mark the maximum and minimum values excluding outliers. The gray thick line represents the mean for healthy controls. Black thick lines represent the mean of each corresponding group. Wilcoxon p values for overall comparison and pairwise comparisons are shown. Bonferroni-adjusted significance level required $p < 0.005$.

marked increase of lactate-to-pyruvate ratio in G1 PAH, which identifies a shift to glycolysis and less oxidative metabolism *via* TCA cycle, as described in prior studies (Fessel et al., 2012; Fijalkowska et al., 2010; Tuder et al., 2012; Xu et al., 2021; Xu et al., 2007).

Metabolic pathways associated with mitochondrial function

To further explore metabolic pathways associated with the change in mitochondrial transmembrane potential and superoxide production, untargeted metabolomics of circulating metabolites is correlated to mitochondrial measures. A total of 22 known metabolites are associated with transmembrane potential in PH at false discovery rate (FDR) < 0.05. Most of these metabolites are in the fatty acid metabolic pathways. The interaction effect of PH group on the metabolite–transmembrane potential relationships is significant in 16 metabolites when comparing G1 with G2 or G3 (FDR < 0.05). These metabolites are also primarily in the fatty acid pathways.

Pathways associated with transmembrane potential in G1 compared with G2 and G3 include fatty acid acyl carnitine metabolism, fatty acid dicarboxylate and monohydrate, as well as androgenic steroids and corticosteroids (FDR < 0.05). Acyl carnitine pathways, which are important in fatty acid oxidation, have the highest fraction of differential metabolites (Table 4). The top two metabolites in the pathway that interact differently with transmembrane potential in G1 *versus* G2–3 are octadecenediacylcarnitine (C18:1-DC) (FDR = 0.005) and suberoylcarnitine (C8-DC) (FDR = 0.01). In addition, fatty acid (acyl carnitine, dicarboxylate) metabolism and dicarboxylate metabolites are significantly different among PH groups and controls (Table 5).

In the overall PH cohort, only four known metabolites associate with changes in mitochondrial superoxide production (FDR < 0.05). Of these, two are xenobiotics, one is involved in lysine metabolism and the other in tryptophan metabolism. There are no significant associations between mitochondrial superoxide production and metabolites at FDR < 0.05 within G1, 2, or 3 PH. No metabolites are significantly associated with mitochondrial mass in the overall PH cohort or within PH groups (all FDR > 0.1). Findings suggest that the mitochondrial transmembrane potential across most PH groups is most strongly associated with changes in fatty acid metabolism.

Mitochondrial function and clinical outcomes

Longitudinal clinical outcomes of death or transplantation of individuals with PH are available for a minimum of 4 years after enrollment to the PVDOMICS study. Mitochondrial measures are not associated with clinical outcomes in the overall PH cohort; however, transmembrane potential is a strong predictor of clinical outcomes of death or transplantation only in G1 PAH, not in the other PH groups. Patients with G1 PAH who die or receive lung transplantation have lower mitochondrial transmembrane potential after adjusting for age, sex, race, and time since diagnosis and the use of PH-specific therapies. The measured transmembrane potential in the 44 individuals who died or had transplantation was 2.8 (2.1, 3.7) mean fluorescence intensity (MFI) $\times 10^4$ *versus* 3.3 (2.3, 4.7) in the 158 individuals without death/transplant (odds ratio: 0.98 [95% confidence interval: 0.96–1.00]; $p = 0.04$). A survival analysis was performed to test for predictors of death or transplantation using Cox proportional hazards regression models. The variables in the analysis are sex, age, use of PH medications, REVEAL LITE 2.0, and mitochondrial transmembrane potential (or superoxide production or mitochondrial mass). In G1 PAH only, higher transmembrane potential is associated with longer transplant-free survival (Fig. 5). Transmembrane potential is not a predictor of survival in G2 or 3 PH. In addition, superoxide production and mitochondrial mass are not associated with survival in any of the PH groups.

Discussion

This is the first study measuring mitochondrial function and mass in a large cohort of PH patients and across all five PH groups in comparison with healthy controls. We show alterations in mitochondrial function as well as decreased arginine bioavailability in PH. Decreased arginine bioavailability is found across all PH groups; however, the alterations in mitochondrial function are more characteristic of G1 PAH

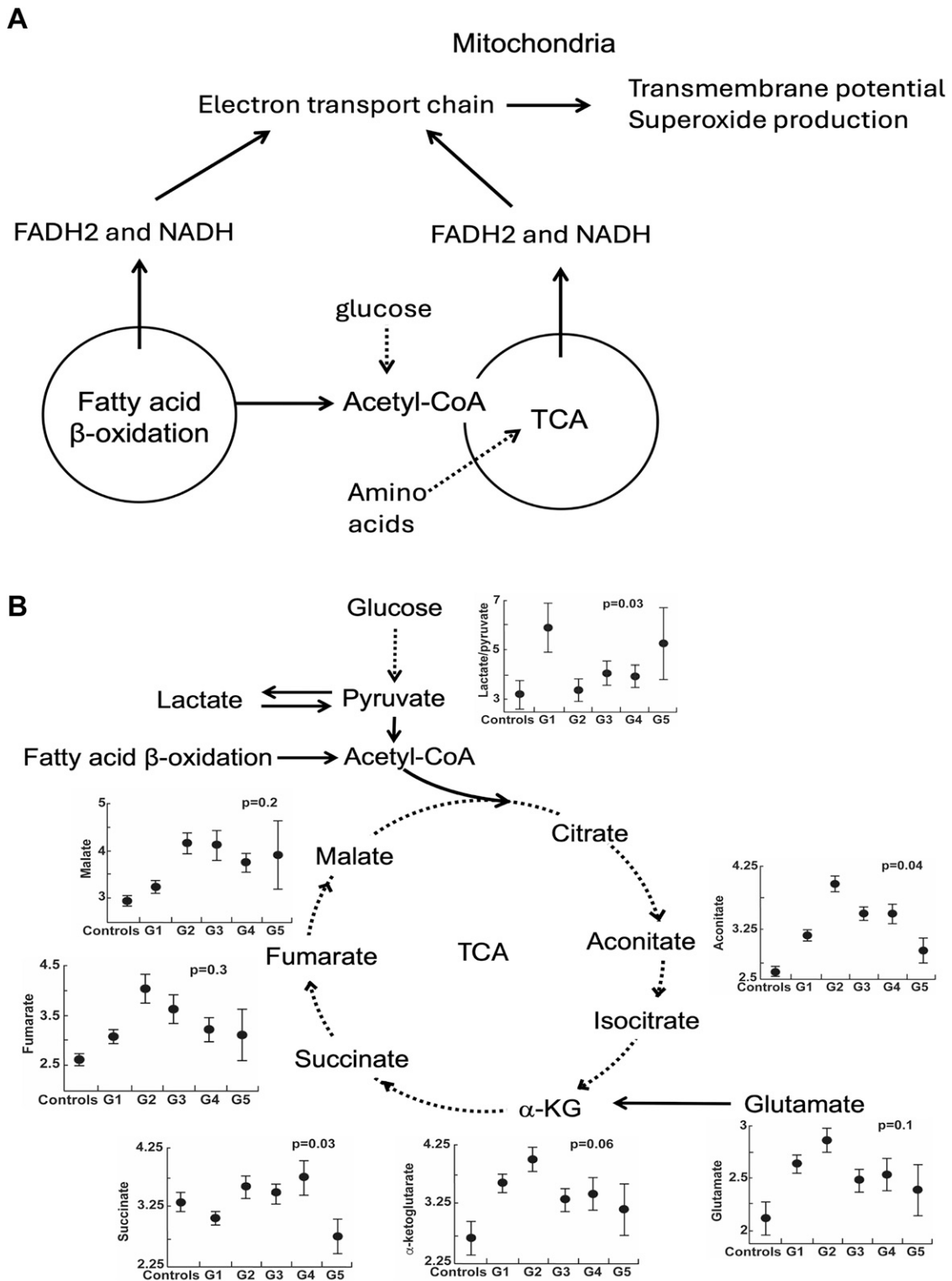


FIG. 4. Mitochondrial electron transport chain (ETC) and the tricarboxylic acid (TCA) cycle. (A) ETC, a series of protein complexes in the inner mitochondrial membrane, picks electrons from reduced electron carriers (NADH/FADH₂) produced by the TCA cycle and fatty acid β -oxidation creating an electrochemical gradient that leads to the production of ATP. Superoxide is produced during the process. Fatty acid β -oxidation transfers electrons to the ETC directly through complex III or by generating acetyl-coA that goes into the TCA cycle. (B) TCA cycle metabolites are different among PH groups and controls with an elevated lactate-to-pyruvate ratio noted in G1 PAH. Data shown as mean with Standard Error of the Mean (SEM). *p* Value adjusted for age, race, sex, and estimated glomerular filtration rate (eGFR).

TABLE 3. TRICARBOXYLIC ACID METABOLITES (UNTARGETED) ACROSS PULMONARY HYPERTENSION GROUPS AND CONTROLS

	Controls	G1 PAH	G2 PH	G3 PH	G4 PH	G5 PH	FDR
Lactate	3.53 [2.81, 4.48]	3.05 [2.33, 3.66]	3.23 [2.71, 4.05]	3.39 [2.63, 4.39]	3.36 [2.66, 3.77]	3.07 [2.50, 4.39]	0.01
Pyruvate	1.66 [1.04, 2.54]	1.00 [0.51, 1.83]	1.44 [0.74, 2.92]	1.11 [0.64, 2.13]	1.04 [0.63, 1.66]	1.18 [0.33, 2.70]	0.05
Succinate	3.23 [2.71, 3.89]	2.90 [2.38, 3.71]	3.56 [2.96, 4.46]	3.33 [2.62, 4.28]	3.43 [2.81, 4.60]	2.68 [2.42, 3.37]	0.03
Aconitate	2.49 [2.22, 3.93]	2.97 [2.40, 3.72]	3.90 [3.27, 4.42]	3.33 [2.75, 4.25]	3.46 [2.91, 4.05]	2.97 [2.28, 3.57]	0.04
2-Methylcitrate/homocitrate	0.85 [0.04, 1.50]	1.21 [0.14, 1.98]	1.59 [1.12, 2.74]	1.31 [0.08, 1.88]	1.09 [0.38, 1.90]	1.58 [1.02, 2.57]	0.01
Glutamate	1.88 [1.13, 2.61]	2.42 [1.81, 3.13]	2.79 [2.16, 3.40]	2.26 [1.71, 3.15]	2.45 [1.76, 3.02]	2.30 [1.61, 2.59]	0.1
Malate	2.83 [2.45, 3.23]	2.85 [2.28, 3.81]	3.77 [2.93, 4.66]	3.26 [2.78, 4.23]	3.83 [2.95, 4.22]	2.95 [2.52, 3.70]	0.2
Fumarate	2.45 [1.98, 2.98]	2.68 [2.04, 3.63]	3.52 [2.75, 4.54]	2.82 [2.23, 3.76]	3.10 [2.41, 3.75]	2.43 [2.05, 3.36]	0.3
α -Ketoglutarate	2.36 [2.02, 3.04]	2.56 [2.05, 3.56]	3.58 [2.92, 4.57]	2.95 [2.47, 4.97]	2.88 [2.46, 3.86]	2.86 [1.96, 3.07]	0.06

Statistics presented as median [P25, P75], FDR across all groups adjusted for age, sex, race, eGFR. FDR, false discovery rate; eGFR, estimated glomerular filtration rate.

patients with decreased transmembrane potential compared with controls and other PH groups, associated with higher superoxide production and changes in fatty acid metabolism. Importantly, mitochondrial transmembrane potential is a predictor of transplant-free survival in G1 PAH, with higher levels associated with better clinical outcomes.

Platelet mitochondrial function has been investigated in various medical conditions (Guo et al., 2009; Rezanian et al., 2017; Shi et al., 2008). In neurological diseases, specific alterations in ETC activity in platelets are found in Alzheimer's disease, Huntington's disease, schizophrenia, migraine headaches, and Parkinson's disease (Ben-Shachar et al., 2007; Parker et al., 1990a, 1990b; Parker et al., 1989; Sangiorgi et al., 1994; Shi et al., 2008). In PH, there are only three studies that looked at platelet bioenergetics. In two separate studies, Nguyen et al. found that platelets from PAH patients had increased glycolysis and higher maximal uncoupled respiration with increased respiratory reserve capacity compared with control platelets, whereas G2 PH platelets did not have increased glycolysis but demonstrated an increased mitochondrial reserve capacity (Nguyen et al., 2017; Nguyen et al., 2019). Interestingly, there is no difference in platelet basal respiration and oxidant production between PH and controls (Nguyen et al., 2017). The authors showed that the increase in reserve capacity is driven by fatty acid oxidation in PAH platelets. In another report comparing PAH patients with healthy controls, G2 PH patients, and participants who had dyspnea but no PH, platelets from PAH patients have increased basal glycolysis and decreased glycolytic reserve compared with platelets from healthy controls, but no difference in the glycolytic rate compared with G2 PH and/or with patients with dyspnea and no PH (McDowell et al., 2020). Smits et al. analyzed platelet ribonucleic acid (RNA) and showed that platelet RNA signatures distinguish PH patients from controls supporting the use of circulating platelets in early diagnosis of patients with PH and as a disease biomarker (Smits et al., 2022). Altogether, the findings support that platelet bioenergetics is altered in PH and could be used as a disease biomarker. It remains unclear whether platelet mitochondrial function reflects the pulmonary vasculature and right ventricle (RV). Further studies are needed to determine if abnormalities of platelet bioenergetics play a role in the pathogenesis of disease or are a result of the known vascular injury/remodeling and thrombotic disease progression.

The ETC spans the inner mitochondrial membrane and comprises four complexes that work together to transfer electrons from NADH and FADH₂ to oxygen (O₂). During this process, protons are pumped by Complexes I and III into the intermembrane space creating a proton gradient that powers Adenosine Triphosphate (ATP) synthesis *via* Complex V. The TCA cycle and fatty acid oxidation are essential sources for NADH and FADH₂. Thus, mitochondrial ETC activity is closely linked to fatty acid oxidation and TCA cycle. All must cooperate to provide the energy needed for cell functions. In this study, while there are no associations between transmembrane potential and TCA pathway metabolites, there are differences in TCA metabolites among PH and controls and a much higher lactate-to-pyruvate ratio in G1 PAH. This confirms a shift to glycolysis, with less pyruvate oxidation in PAH (Xu et al., 2021). In contrast, transmembrane potential is associated with fatty acid pathways, that is, fatty acyl carnitine

TABLE 4. FATTY ACID METABOLISM PATHWAYS AND METABOLITES ASSOCIATED DIFFERENTIALLY WITH MITOCHONDRIAL TRANSMEMBRANE POTENTIAL IN GROUP1 VERSUS GROUPS 2–3 PULMONARY HYPERTENSION

Pathway	Metabolite	TDP	FDR
Fatty acid (acyl carnitine, dicarboxylate) metabolism	Octadecenediylcarnitine (C18:1-DC)	0.4	0.009
	Suberoylcarnitine (C8-DC)		0.005
Fatty acid, dicarboxylate	Hexadecenedioate (C16:1-DC)	0.16	0.01
	Hexadecanedioate (C16)		0.005
	Octadecenedioate (C18:1-DC)		0.04
	Tetradecanedioate (C14)		0.04
	Octadecanedioate (C18)		0.05
	3-Hydroxydodecanedioate		0.07
	Tetradecadienedioate (C14:2-DC)		0.07
	3-Hydroxyadipate		0.09
Fatty acid, monohydroxy	3-Hydroxyhexanoate	0.17	0.04
	3-Hydroxysebacate		0.01
	16-Hydroxypalmitate		0.01
			0.03

TDP represents the proportion of truly different metabolites in the pathway. FDR represents the comparison of the association of pathway or metabolite with transmembrane potential in G1 compared with G2–3 PH. Model adjusted for age, race, sex, eGFR, and PH medications. TDP, true discovery proportion; G1, group 1; G2–3, groups 2–3.

dicarboxylate metabolism. Fatty acyl carnitine dicarboxylate metabolism enables transport and processing of long-chain fatty acids into the mitochondria for oxidation. Inside the mitochondria, fatty acyl carnitine is converted to fatty acyl CoA, which is broken down through β -oxidation for the generation of NADH and FADH₂. The findings in this study suggest that G1 PAH may have increased reliance on fatty acid oxidation for energy, and preference for entry of reducing equivalents directly into Complex III (Gnaiger, 2024).

Imbalance in different types of ROS is well described in PH and linked to pathogenesis (Breault et al., 2023; Sutendra and Michelakis, 2014). Previous studies measured hydrogen peroxide in the pulmonary vasculature of hypoxic and nonhypoxic PH models and found different results based on experimental conditions, species, and hypoxic conditions emphasizing the complexity of mitochondrial ROS changes related to disease stage, etiology, species/model, and tissue studied (Afolayan et al., 2016; Archer et al., 2010; Archer et al., 2008; Bonnet et al., 2006; Chi et al., 2010; Nozik-Grayck et al., 2008; Waypa et al., 2010). Mitochondrial number or mass, which controls cellular bioenergetic capacity, was shown to be reduced in the skeletal muscle of PH patients and in the pulmonary vasculature and RV of rat models of PH (Archer et al., 2008; Bonnet et al., 2006; Nisoli and Carruba, 2006; Xu et al., 2007). Nguyen et al. found no difference in mitochondrial superoxide production in platelets from G1 PAH, G2 PH, and controls (Nguyen et al., 2017; Nguyen et al., 2019). In this study, G1 PAH has higher superoxide production compared with G3 PH and controls. This suggests that the metabolic mechanisms underlying PAH differ from those of G3 PH.

The study has limitations. One important limitation is the difficulty in accounting for the effect of disease duration and PH therapies on platelet mitochondrial function and more so the specific therapeutic subclasses. Studies investigating platelet mitochondrial function over time and in response to therapy are warranted to help understand the effect of PH therapies and disease progression on platelets. Based on our findings, it is

difficult to determine if the changes in platelet mitochondrial function are a cause or an effect of PH. Nonetheless, the differences in mitochondrial function among the PH groups suggest that it is linked to disease pathogenic mechanisms. Extrapolating from studies in heart failure (Rosca and Hoppel, 2010), mitochondrial dysfunction could be both the cause and the result of disease pathogenesis leading to metabolic reprogramming, increased oxidative stress, and RV failure. Another limitation is the lack of platelet functional mechanistic assays, which were beyond the scope of the current study. G4 and 5 PH was underrepresented in our cohort and a larger sample size is needed to better characterize mitochondrial mass and function in these two groups. Another important modulator of mitochondrial function that was not accounted for in this study is the loss of bone morphogenetic protein receptor type II function and its association with mitochondrial dysfunction and oxidative stress in PH (Cuthbertson et al., 2023; Diebold et al., 2015; Egnatchik et al., 2017; Lane et al., 2011).

In summary, decreased arginine bioavailability is found in all PH groups; whereas mitochondrial functions vary among PH groups. Lower transmembrane potential with increased superoxide production is a unique characteristic of G1 PAH and is associated with changes in fatty acid metabolism. The transmembrane potential is predictive of clinical outcomes in G1 PAH. The G1 PAH findings are in contrast to G3, where superoxide is lower and transmembrane potential is higher, suggesting different metabolic states among these groups. Further studies are needed to investigate mitochondrial mechanisms in all PH and to identify targets for specific metabolic interventions to improve clinical outcomes.

Materials and Methods

Study population and sample collection

The PVDOMICS study is an observational prospective longitudinal cohort (clinicaltrials.gov NCT02980887). The study protocol and a STROBE diagram depicting enrollment

TABLE 5. DIFFERENCES IN FATTY ACID METABOLITES (ACYL CARNITINE, DICARBOXYLATE METABOLISM, AND DICARBOXYLATE PATHWAY) ACROSS PULMONARY HYPERTENSION GROUPS AND CONTROLS

Pathway	Metabolite	Controls	G1 PAH	G2 PH	G3 PH	G4 PH	G5 PH	FDR
Fatty acid (acyl carnitine, dicarboxylate) metabolism	Octadecenylcarnitine (C18:1-DC)	0.9 [0.6, 1.4]	1.7 [1.1, 2.6]	2.3 [1.3, 2.3]	2.0 [1.2, 3.0]	2.1 [1.3, 2.8]	1.6 [1.0, 2.1]	<0.001
	Subterylcarnitine (C8-DC)	0.5 [0.1, 0.7]	1.4 [0.7, 2.5]	1.9 [1.1, 3.1]	1.3 [0.9, 2.6]	1.3 [0.8, 1.9]	0.8 [0.4, 2.4]	<0.001
	Hexadecenylcarnitine (C16:1-DC)	1.6 [1.2, 1.8]	2.1 [1.7, 3.0]	2.3 [1.6, 3.7]	2.3 [1.5, 3.2]	2.3 [1.3, 3.4]	1.6 [1.1, 2.7]	<0.001
Fatty acid, dicarboxylate	Hexadecanedioate (C16)	1.1 [0.7, 1.6]	1.7 [1.2, 3.0]	1.9 [1.3, 3.6]	2.2 [1.5, 3.4]	2.0 [1.1, 3.4]	1.3 [1.0, 2.7]	<0.001
	Octadecanedioate (C18:1-DC)	1.4 [0.9, 1.9]	1.9 [1.3, 2.9]	2.1 [1.3, 3.3]	2.1 [1.6, 2.9]	2.3 [1.2, 2.7]	1.8 [1.2, 3.2]	0.03
	Tetradecanedioate (C14)	1.1 [0.7, 1.6]	1.7 [1.1, 2.6]	1.7 [1.1, 2.8]	1.9 [1.1, 2.8]	1.8 [1.3, 2.7]	1.7 [1.0, 2.4]	<0.001
	Octadecanedioate (C18)	1.2 [0.8, 1.8]	1.7 [1.1, 2.7]	1.8 [1.2, 2.9]	2.1 [1.5, 2.9]	1.9 [1.5, 3.2]	1.9 [1.2, 2.4]	0.03
	3-Hydroxydodecanedioate	0.5 [0.1, 0.9]	1.2 [0.5, 2.1]	1.4 [0.7, 2.8]	1.3 [0.7, 2.7]	1.2 [0.7, 2.7]	1.0 [0.4, 1.7]	0.01
	Tetradecanedioate (C14:2-DC)	1.2 [0.6, 1.7]	1.6 [0.9, 2.6]	1.8 [1.2, 3.0]	1.7 [0.9, 2.7]	1.7 [1.0, 3.0]	1.1 [0.7, 1.8]	<0.001
	3-Hydroxyadipate	0.6 [0.5, 1.0]	1.2 [0.7, 2.3]	1.8 [1.1, 3.0]	1.5 [0.8, 2.3]	1.2 [0.7, 1.7]	1.0 [0.5, 1.6]	0.1

Values for metabolites are shown as median [P25, P75]. FDR comparing metabolites across PH group and controls adjusting for age, sex, race, and eGFR.

and patient classification have been previously published (Hemnes et al., 2022). The study was approved by the Institutional Review Board of the Cleveland Clinic and all clinical sites enrolling participants. It was sponsored by the National Institutes of Health Heart, Lung and Blood Institute and the Pulmonary Hypertension Association. Written informed consent was obtained from all individuals. Incident and prevalent patients with PH, disease comparators, and age-, sex-, race-, and Hispanic ethnicity-matched healthy controls were recruited from seven clinical sites across the United States (Hemnes et al., 2022). The present study involved two groups: patients with PH according to the Fifth World Symposium on Pulmonary Hypertension guidelines with mean pulmonary arterial pressure (mPAP) ≥ 25 mmHg and healthy control subjects with normal cardiopulmonary findings and without end-organ disease. All participants were ≥ 18 years old. The inclusion criteria for patients with PH were the following: age ≥ 18 years, referred for right heart catheterization for clinical purposes, able to perform complete diagnostic testing, treatment naive, or prior drug exposure. Exclusion criteria were end-stage renal disease requiring renal replacement therapy, too ill to perform study protocol, pregnant or nursing, and active malignancy other than nonlocalized skin cancer. Following right heart catheterization, PH participants were classified according to the 2013 World Symposium on Pulmonary Hypertension guidelines that were in effect at the inception of the study (Simonneau et al., 2013). PH was defined by right heart catheterization, as mPAP ≥ 25 mmHg, and PAH was defined as mPAP ≥ 25 mmHg, and pulmonary vascular resistance > 3 Wood Units with pulmonary artery wedge pressure ≤ 15 mmHg. Patients were assigned PH groups based on the five recognized groups of disorders that cause PH: PAH (G1); PH due to left heart disease (G2); PH due to chronic lung disease and/or hypoxia (G3); chronic thromboembolic PH (G4); and PH due to unclear multifactorial mechanisms (G5). Subjects were classified as single or mixed etiology PH at the discretion of the site principal investigator. For this study, analysis was performed using the single etiology PH group unless otherwise specified. Participants were assigned to appropriate groups by investigators with the oversight of an Adjudication Committee. Healthy controls underwent all non-invasive testing and blood sampling but did not undergo right heart catheterization or ventilation/perfusion scanning. Comprehensive clinical phenotyping was performed through standardized cardiopulmonary testing, including pulmonary function testing, 6-minute walk distance (6MWD) testing, echocardiography, cardiac magnetic resonance imaging, resting right heart catheterization with O₂, and vasodilator challenge followed by fluid challenge or invasive cardiopulmonary exercise testing and measurement of N-terminal pro-brain natriuretic peptide (NT-proBNP) as previously described (Hemnes et al., 2022). REVEAL LITE 2.0 risk was calculated by incorporating NT-proBNP, 6MWD, the World Health Organization functional class, systolic blood pressure, heart rate, and estimated glomerular filtration rate (eGFR) (Benza et al., 2021). Peripheral venous blood was collected in BD Vacutainer 4 mL sodium-heparin blood tubes (BD, Cat# 367871, San Jose, CA) and processed the following morning after overnight shipment to the Cleveland Clinic from the other study institutions. Samples were

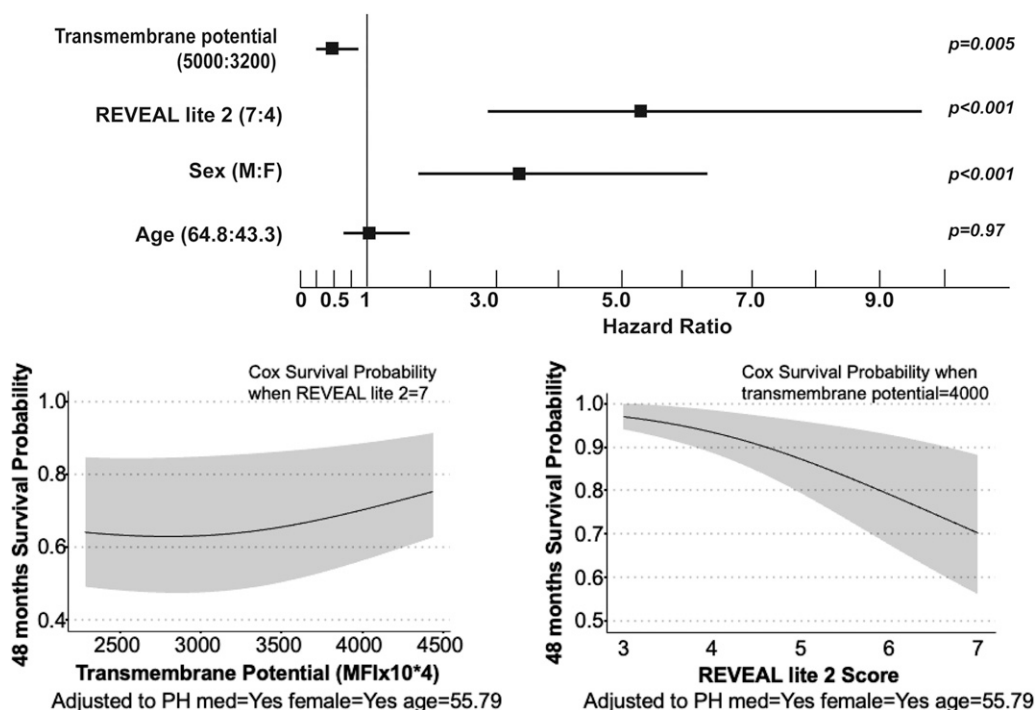


FIG. 5. Mitochondrial transmembrane potential is a predictor of survival in G1 PAH. We performed Cox proportional hazard survival analysis to predict clinical outcomes using predictors age, sex, REVEAL LITE 2, and transmembrane potential. Only in G1 PAH, transmembrane potential was a predictor of survival (hazard ratio = 0.45 [0.25–0.79], $p = 0.009$). Forty-eight months of survival plots are shown for transmembrane potential and REVEAL LITE 2 score. In contrast to REVEAL LITE 2, which demonstrates a robust predictive value for survival across its entire range, transmembrane potential exhibits a nonlinear association. Specifically, at lower values, the survival curve remains relatively flat, while at higher transmembrane potential values ($>3000\text{--}3500 \times 10^4$), there is a significant association with improved survival.

not stored. Hemolyzed samples were excluded and a total of 767 samples were processed. All samples were deidentified. Electronic laboratory notebook was used.

Measurement of mitochondrial function and mass by flow cytometry

Mouse splenocyte reference sample preparation. Mouse splenocyte reference samples were used daily to help ensure that flow cytometry data acquisition each day was not impacted by flow cytometer setup, sample preparation, staining, or any other variables. Acceptable reference ranges for MFI of each mitochondrial probe were calculated following three consecutive days of data acquisition using batches of isolated mouse splenocytes frozen in liquid nitrogen, with average MFI ± 2 standard deviation (SD) determining the reference range. Mouse splenocyte reference samples were stained and run daily with the test platelet samples.

Isolation and processing of platelets from whole blood. Blood tubes were inverted to gently mix following shipment and centrifuged at 150 g for 20 min with the brake turned off. The yellow layer of platelet-rich plasma was carefully collected from each tube using a 1 mL micropipette and transferred into a 15 mL polyethylene tube. For each milliliter of platelet-rich plasma collected, 1 μ L of 10 mM prostaglandin E1 (PE1) was added. PE1 is used to inhibit platelet aggregation (Xu et al., 2015). Platelet-rich plasma was centrifuged

at 150 g for 10 min to avoid red blood cell contamination that may have been inadvertently included in the platelet-rich plasma following the initial centrifugation. The supernatant was transferred into a new 15 mL polyethylene tube. This suspension was centrifuged at 1500 g for 15 min with the acceleration and brake both set to maximum. Platelet pellets were resuspended in 1 mL of Tyrode’s buffer/PE1. Platelets were counted using a TC20 Cell Counter (Bio-Rad, Cat#145–0102, Hercules, CA).

Mitochondrial function flow cytometry assay. Platelet pellets in four of the five mini flow tubes were resuspended in 90 μ L of Tyrode’s buffer/PE1. The platelet pellet in the fifth tube was resuspended in 90 μ L of 20 μ M FCCP (carbonyl cyanide *p*-trifluoromethoxyphenylhydrazine) in Tyrode’s buffer/PE1 and incubated for 10 min. Each of the five tubes then received an additional 10 μ L of specific MitoProbe dilutions to reach a final volume of 100 μ L. All MitoProbe had a stock concentration of 1 mM. One tube was an unstained control and therefore only received an additional 10 μ L of Tyrode’s buffer/PE1. One tube resuspended in Tyrode’s buffer/PE1 and the tube treated with FCCP/Tyrode’s buffer/PE1 received 10 μ L of a 1/250 dilution of TMRE (tetramethyl rhodamine, ethyl ester, Abcam, Cat#113852, Cambridge, UK) for a final dilution of 1/2500 TMRE. One tube received 10 μ L of a 1/100 dilution of MitoTracker Green (Invitrogen, Cat#M7514, Waltham, MA) for a final dilution of 1/1000 MitoTracker Green. The final tube received 10 μ L of a 1/25 dilution of MitoSOX

Red (Invitrogen, Cat#M36008, Waltham, MA) for a final dilution of 1/250. Resuspend platelets and incubate in the dark for 30 min at 37°C. Following incubation, 1 mL of Tyrode's buffer/PE1 was added to the four tubes without FCCP and 1 mL of FCCP/Tyrode's buffer/PE1 for the tube that previously received FCCP. All tubes were centrifuged at 3100 g for 4 min and platelet pellets were resuspended in 250 µL of Tyrode's buffer/PE1 (250 µL FCCP/Tyrode's buffer/PE1 for FCCP tube). Samples were stored in the dark with the unstained, MitoTracker Green, and MitoSOX Red samples at 4°C and the TMRE and TMRE/FCCP samples at 37°C until data acquisition.

Data acquisition on flow cytometer. Data acquisition was performed on a BD LSR Fortessa Flow Cytometer (BD, San Jose, CA) using a blue laser (Ar488) with a 515/20 filter for MitoTracker Green, blue laser (Ar488) with an LP535 dichroic and 585/42 filter for MitoSOX Red, and a yellow green laser (561) with 582/15 filter for TMRE. The six peak SHERO Ultra Rainbow Calibration Kit (Spherotech, Cat#URCP-50-2K, Lake Forest, IL) was used to standardize fluorescence detectors. A total of 50,000 events were acquired for all platelet tubes and 10,000 events were acquired for all mouse splenocyte reference sample tubes. Data were saved as Flow Cytometry Standard (FCS) files on the institutional server.

Data analysis

Data analysis was performed using FlowJo X software by investigators blinded to the diagnosis associated with the samples. All raw data acquired for each sample were displayed on forward scatter or FSC-A × FSC-H light scatter and gated tightly along the diagonal axis for aggregate exclusion. This population was then displayed on side scatter or SSC-A × SSC-H light scatter and gated tightly along the diagonal axis for debris exclusion. These gated single platelet events were then evaluated for fluorescence, and MFI was calculated in the channel corresponding to each probe (Data acquisition on flow cytometer), using the following gating strategies (Supplementary Fig. S1).

For MitoTracker Green-stained samples, no further gating was used and all single platelet events were used to calculate MFI in Blue-515, measuring the mitochondrial mass present in each individual sample. Unstained single platelet MFI in Blue-515 was subtracted from the MFI of the MitoTracker Green-stained single platelets for background correction. Thirty-one samples showed significant populations with negative fluorescence in Blue-515 and were excluded due to this abnormal fluorescent signal. Fourteen samples had single platelet event counts <5000 and were excluded due to insufficient events for accurate flow cytometric analysis.

For MitoSOX Red-stained samples, MitoSOX Red-positive events were gated in Blue-710 and the MFI of this population was calculated to measure superoxide presence within the platelets. Unstained single platelet MFI in Blue-710 was subtracted from the MFI of the MitoSOX Red-stained single platelets for background correction. Four samples had distorted light scatter inconsistent with MitoSOX Red fluorescent signals indicating sample degradation and were excluded. One sample had only 1000 total single platelet events collected and

was excluded. One sample was contaminated with TMRE and was excluded.

For TMRE-stained samples, TMRE-positive events were gated in YG-582 and the MFI of this population was calculated, measuring mitochondrial transmembrane potential in the samples. MFI in YG-582 of all single platelet events from the TMRE+FCCP sample was subtracted from the MFI of the TMRE-stained single platelets for background correction. One sample had no TMRE signal measured due to possible MitoSOX Red contamination and was excluded. One sample had an abnormal signal in the TMRE+FCCP tube used for background correction and the sample was excluded. One sample had no TMRE data collected and was therefore excluded.

In total, 767 samples were collected and prepared for data acquisition on the flow cytometer. Forty-three samples had MitoTracker Green data excluded, leaving a total of 724 data points. Six samples had MitoSOX Red data excluded, leaving a total of 761 data points. Three samples had TMRE data excluded, leaving a total of 764 data points. A total of 717 samples have data points for all three stains. Background-adjusted MFIs for all nonexcluded samples were reported.

Mitochondrial probe MFI of mouse splenocyte reference samples had to fall within the established reference range for the platelet data to be included in our final analysis.

Arginine-NO metabolism

Plasma amino acid and urinary nitrate analysis. Plasma arginine, citrulline, and ornithine concentrations were measured using high-performance liquid chromatography (HPLC; Agilent 1100 series HPLC; Agilent Technologies; Wilmington, DE), following ortho-phthalaldehyde derivatization using a fluorescent detector as described previously (Kalhan et al., 2003).

Nitrate in urine samples was measured to assess whole-body NO production (Castillo et al., 1993). Urine nitrate was measured using the ENO-30, a dedicated HPLC system (Amuza, San Diego, CA). Urine was diluted 1:50 in the analyzer carrier solution before running. Urine samples were also screened for the presence of nitrite (*i.e.*, urinary tract microbial infection) with the Griess reaction, and samples testing positive for nitrite were excluded from analysis. Urine creatinine was measured in all samples, and nitrate concentration was normalized to creatinine concentration.

Nontargeted metabolomic analysis. Nontargeted metabolomic and lipidomic analyses were performed at Metabolon, Inc. (Durham, NC). The details of analytical platform and data curation have been described in detail previously (Comhair et al., 2015). The global, unbiased platform was based on a combination of three separate platforms: ultrahigh performance liquid chromatography/tandem mass spectrometry (UHPLC/MS/MS) optimized for basic species, UHPLC/MS/MS optimized for acidic species, and gas chromatography/mass spectrometry (GC/MS). The major components of the analytic process and the analytic platform have been described in detail in previous publications (Comhair et al., 2015; Evans et al., 2009; Kalhan et al., 2011). UHPLC/MS/MS analysis utilized a Waters Acquity UHPLC (Waters Corporation, Milford, MA) coupled to an Linear Trap Quadrupole (LTQ) mass spectrometer (Thermo Fisher Scientific, Inc., Waltham, MA) equipped with an electrospray ionization

source. Two separate injections were performed on each sample: one optimized for positive ions and one for negative ions. Derivatized samples for GC/MS were analyzed on a Thermo-Finnigan Trace DSQ fast-scanning single-quadrupole MS operated at unit mass resolving power. Chromatographic separation followed by full-scan mass spectra was carried to record retention time, mass-to-charge (m/z) ratio, and MS/MS of all detectable ions present in the samples. Compounds were identified by automated comparison with Metabolon's reference library entries. Identification of known chemical entities was based on comparison with Metabolon's library entries of purified standards.

Statistical analysis

Quantitative variables were summarized with means and SDs or medians and interquartile ranges as appropriate depending on skewness, while categorical variables were summarized as frequencies and percents. Group comparisons were done using Pearson's chi-square or Fisher's exact test for categorical variables. We used analysis of variance or Kruskal-Wallis for continuous variables at 0.05 significance levels, with pairwise group comparisons performed with two-tailed t -tests or Wilcoxon test as appropriate at Bonferroni-adjusted significance levels to account for multiple comparisons. Pearson's correlations were used to assess the relationships between continuous variables and a line of best fit used in figures for visualization. Multivariable regression models were used to test the differences in mitochondrial measures comparing healthy controls and PH adjusting for age, sex, and race. To adjust for PH medications, propensity scores were calculated using the Inverse Probability Treatment Weighting (IPTW) method. Sex, age, and race were used as confounders. Generalized linear models adjusted for PH medications were used to test the differences of the mitochondrial measures between the PH groups. Bonferroni-adjusted significance level <0.005 for multiple comparisons were reported. Analyses were performed on the data as of January 30, 2023, using JMP Pro, version 17.0 (SAS Institute) and SAS software (version 9.4, Cary, NC).

Statistical Analysis of Untargeted Metabolomics

Filtering and scaling

Baseline venous plasma untargeted metabolomic data from Metabolon were filtered per metabolite using all PVDOMICS participants so that the remaining metabolites had $<50\%$ missing values and their ratio of median absolute deviation (MAD)-to-median value was ≥ 0.25 . Each metabolite was rescaled to have an MAD and median of 1 using all PVDOMICS participants. Filtered and scaled metabolite data were then subsetted to those with PH or healthy controls and complete platelet mitochondrial mass and mitochondrial function data.

Imputation of clinical covariates

Missing data in key clinical covariates, eGFR (46 missing), race (13 missing), PH medication use (3 missing), and body mass index (BMI) (2 missing) were imputed using Random Forest imputation (Stekhoven and Buhlmann, 2012) and additional complete predictors recruiting center, gender, age, PH status, PH group, mitomass, and mitochondrial function, and

50 principal components from the scaled, filtered, and subsetted metabolite data after \log_2 transformation.

Differential metabolite abundance

Differential metabolite abundance analyses were performed per metabolite using a robust and efficient semiparametric regression modeling approach (Liu et al., 2017) with a log-link. Additive regression models per metabolite (outcome) were fit using maximum likelihood and the PH-only subset (all PH groups) with covariate adjustment for recruiting center, gender, age, BMI, eGFR, race, PH medication use, PH group, and platelet mitochondrial mass, transmembrane potential, or superoxide production. Age, BMI, eGFR, and mitochondrial variables were included as 2 degree-of-freedom restricted cubic splines to allow for nonlinear effects. p Values per mitochondrial predictor were calculated using likelihood-ratio tests, then adjusted per predictor to get FDR-controlled values using the Benjamini-Hochberg method (Benjamini and Hochberg, 1995). Effect sizes of mitochondrial predictors on metabolites were calculated by assessing the change in predicted median metabolite values as the mitochondrial predictor changed (typically from its first to third quartile), while all other predictors in the model remained constant at a specified value (typically at their modal or median values).

To assess interaction effects of PH group on the metabolite-mitochondrial measure relationships, the regression models were refit to include a PH group by mitochondrial measure interaction term (both linear and nonlinear) but restricted to PH groups 1-3 due to small sample sizes in PH groups 4 and 5. Overall p values of interaction strength were calculated using likelihood ratio tests, and contrasts of metabolite-mitochondrial relationships in PH 2 or 3 versus PH 1 were estimated. Finally, PH1-3-specific models were fit.

Metabolite pathway analyses were conducted for each of the models using the corresponding individual metabolite-mitochondrial association p values as inputs, the Metabolon-provided pathway annotations, and the principled R-package Simultaneous Enrichment Analysis (rSEA) method (Ebrahimipour et al., 2020). The competitive null hypothesis of a higher true discovery proportion (TDP) for metabolites in the pathway versus outside the pathway was tested for every pathway. The rSEA method controlled the overall family-wise error rate across all possible pathways from the tested metabolites. The estimated TDP was reported for each pathway.

Survival Analysis of Platelet Mitochondrial Measures

Imputation of clinical covariates and survival analyses were done separately within each of the PH groups 1-3. Survival event was composite of death or transplant.

Imputation of clinical covariates

Missing data in clinical covariates defining the REVEAL LITE 2 risk score and key covariates from the metabolite models above were imputed using Random Forest imputation (Stekhoven and Buhlmann, 2012) and additional complete predictors recruiting center, gender, age, PH status, World Symposium on Pulmonary Hypertension (WSPH) group, mitomass and mitochondrial function, death or transplant status, time to death or transplant or last follow-up, and number of years since PH diagnosis.

Survival analysis

Cox proportional hazards models were fit for the composite death or transplant event with noninformative censoring at time of last follow-up applied to those without an event. Baseline hazards were stratified by PH medication use. Covariate model included gender, age, REVEAL LITE 2 score, and platelet mitochondrial mass, transmembrane potential, or superoxide production. Age, REVEAL LITE 2 score, and mitochondrial variables were included as 2 degree-of-freedom restricted cubic splines to allow for non-linear effects. *p* Values per mitochondrial predictor were calculated using likelihood-ratio tests. Effects of mitochondrial predictors on survival were displayed as plots of predicted 4-year survival probabilities as the mitochondrial predictor changed (typically from its first to third quartile), while all other predictors in the model remained constant at a specified value (typically at their modal or median values). Proportional hazard assumptions were checked and tested using Schoenfeld residual plots and tests.

All metabolite and survival analyses were conducted using R version 4.3 and the R packages survival, data.table, rms, and Hmisc.

Acknowledgments

The authors thank the PVDOMICS network and all the participants.

Authors' Contributions

S.F. analyzed and interpreted the data and wrote the article. K.A. designed and performed the research, analyzed and interpreted the data, and reviewed the article. P.M.H. reviewed the article. J.B. helped with metabolomic statistical analysis and plots. S.C. collected data and samples and put in place in the database. A.R. performed flow cytometry and analyzed the data. N.W. performed the experiments. M.R. helped with statistical analysis. S.C.E. designed the research, analyzed the data, and reviewed the article. M.A.A., G.J.B., E.B.-R., B.A.B., R.P.F., G.G., A.R.H., N.H., E.M.H., C.J., J.A.L., R.M., M.M.P., F.P.R., and W.H.W.T. reviewed the article. All PVDOMICS investigators recruited, collected samples, and ensured that all testing and data were collected on participants as per the study protocol.

Author Disclosure Statement

A.R.H. has served as a consultant for Bayer, United Therapeutics, Janssen, GossamerBio, and Tenax Therapeutics; holds stock in Tenax Therapeutics; and has received grants from the National Institutes of Health, CMREF, and Imara. J.A.L. is supported by the National Institutes of Health grant U01 125215 and the American Heart Association 19A1ML 34980000; receives salary support from the Massachusetts Medical Society; has received research funding (to her institution) from Astellas; has served as a consultant for Abbott Vascular and United Therapeutics; and has served as a site principal investigator for a study sponsored by Aria CV. E.B.-R. has received consulting fees from Acceleron for a scientific advisory board meeting; and her institution receives grant support from Bayer, United Therapeutics, Janssen, and SonVie. B.A.B. has received research support from the National

Institutes of Health (NIH) and the U.S. Department of Defense, as well as research grant funding from AstraZeneca, Axon, GlaxoSmithKline, Medtronic, Mesoblast, Novo Nordisk, Rivos, and Tenax Therapeutics; and has served as a consultant for Actelion, Amgen, Aria, Axon Therapies, BD, Boehringer Ingelheim, Cytokinetics, Edwards Lifesciences, Eli Lilly, Imbria, Janssen, Merck, Novo Nordisk, NGM, NXT, and VADovations, and is named inventor (US Patent no. 10,307,179) for the tools and approach for a minimally invasive pericardial modification procedure to treat heart failure. J.E.F. is a consultant to Wolters Kluwer Health, Clinical Drug Information Ad Honorem. R.P.F. has consulting, steering committee, and advisory board relationships with Altavant Sciences, Bayer, Gossamer Bio, Janssen, Shouti, France Foundation, IQVIA, Tenax, UpToDate, and United Therapeutics. N.H. has received research grants for Acceleron, Aerovate, Altavant, Gossamer, Liquidia, Merck, and United Therapeutics; and has served on advisory boards for Acceleron, Aerovate, Altavant, Gossamer, and Liquidia. R.M. has received honorarium from the American Academy of Sleep Medicine, funds for service on the American Board of Internal Medicine Sleep Medicine Testing Writing Committee, Associate Editor for the *American Journal of Respiratory and Critical Care Medicine* and has received funding from the NIH and investigator-initiated research funds to her institution from Inspire and Sommetrics and royalties from UpToDate. M.M.P. has served on the Speakers Bureau of Lantheus Medical Imaging (Definity contrast). F.P.R. has consulting relationships with Acceleron and United Therapeutics; is on a Steering Committee for Acceleron; and receives research support from Ismed, United Therapeutics, Bayer, Acceleron, Janssen, and AADI. E.M.H. has served on the Data and Safety Monitoring Board of Trisol, AADI Biosciences, and SoniVie; has served on the Clinical Events Committee for V-wave and the steering committee for Pulnovomed; and has served as a consultant for Biotronik. All other authors have reported that they have no relationships relevant to the contents of this article to disclose.

Funding Information

The study was supported by grants U01 HL125218 (PI: E.B.-R.), U01 HL125205 (PI: R.P.F.), U01 HL125212 (PI: A.R.H.), U01 HL125208 (PI: F.P.R.), U01 HL125175 (PI: P.M.H.), U01 HL125215 (PI: J.A.L.), U01 HL125177 (PI: G.J.B.), RO1 HL060917 (PI: S.C.E.), and the Pulmonary Hypertension Association.

Supplementary Material

Supplementary Figure S1
Supplementary Table S1

References

- Afolayan AJ, Eis A, Alexander M, et al. Decreased endothelial nitric oxide synthase expression and function contribute to impaired mitochondrial biogenesis and oxidative stress in fetal lambs with persistent pulmonary hypertension. *Am J Physiol Lung Cell Mol Physiol* 2016;310(1):L40-L49; doi: 10.1152/ajplung.00392.2014
- Archer SL, Gomberg-Maitland M, Maitland ML, et al. Mitochondrial metabolism, redox signaling, and fusion: A mitochondria-

- ROS-HIF-1 α -Kv1.5 O₂-sensing pathway at the intersection of pulmonary hypertension and cancer. *Am J Physiol Heart Circ Physiol* 2008;294(2):H570–H578; doi: 10.1152/ajpheart.01324.2007
- Archer SL, Marsboom G, Kim GH, et al. Epigenetic attenuation of mitochondrial superoxide dismutase 2 in pulmonary arterial hypertension: A basis for excessive cell proliferation and a new therapeutic target. *Circulation* 2010;121(24):2661–2671; doi: 10.1161/CIRCULATIONAHA.109.916098
- Aytekin M, Aulak KS, Haserodt S, et al. Abnormal platelet aggregation in idiopathic pulmonary arterial hypertension: Role of nitric oxide. *Am J Physiol Lung Cell Mol Physiol* 2012;302(6):L512–L520; doi: 10.1152/ajplung.00289.2011
- Benjamini Y, Hochberg Y. Controlling the false discovery rate: A practical and powerful approach to multiple testing. *J R Stat Soc B Methodol* 1995;57(1):289–300; doi: 10.1111/j.2517-6161.1995.tb02031.x
- Ben-Shachar D, Bonne O, Chisin R, et al. Cerebral glucose utilization and platelet mitochondrial complex I activity in schizophrenia: A FDG-PET study. *Prog Neuropsychopharmacol Biol Psychiatry* 2007;31(4):807–813; doi: 10.1016/j.pnpbp.2006.12.025
- Benza RL, Kanwar MK, Raina A, et al. Development and validation of an abridged version of the REVEAL 2.0 risk score calculator, REVEAL Lite 2, for use in patients with pulmonary arterial hypertension. *Chest* 2021;159(1):337–346; doi: 10.1016/j.chest.2020.08.2069
- Bonnet S, Michelakis ED, Porter CJ, et al. An abnormal mitochondrial-hypoxia inducible factor-1 α -Kv channel pathway disrupts oxygen sensing and triggers pulmonary arterial hypertension in fawn hooded rats: Similarities to human pulmonary arterial hypertension. *Circulation* 2006;113(22):2630–2641; doi: 10.1161/CIRCULATIONAHA.105.609008
- Breault NM, Wu D, Dasgupta A, et al. Acquired disorders of mitochondrial metabolism and dynamics in pulmonary arterial hypertension. *Front Cell Dev Biol* 2023;11:1105565; doi: 10.3389/fcell.2023.1105565
- Castillo L, deRojas TC, Chapman TE, et al. Splanchnic metabolism of dietary arginine in relation to nitric oxide synthesis in normal adult man. *Proc Natl Acad Sci U S A* 1993;90(1):193–197; doi: 10.1073/pnas.90.1.193
- Chi AY, Waypa GB, Mungai PT, et al. Prolonged hypoxia increases ROS signaling and RhoA activation in pulmonary artery smooth muscle and endothelial cells. *Antioxid Redox Signal* 2010;12(5):603–610; doi: 10.1089/ars.2009.2861
- Comhair SA, McDunn J, Bennett C, et al. Metabolomic endotype of asthma. *J Immunol* 2015;195(2):643–650; doi: 10.4049/jimmunol.1500736
- Cuthbertson I, Morrell NW, Caruso P. BMPR2 mutation and metabolic reprogramming in pulmonary arterial hypertension. *Circ Res* 2023;132(1):109–126; doi: 10.1161/CIRCRESAHA.122.321554
- Diebold I, Hennigs JK, Miyagawa K, et al. BMPR2 preserves mitochondrial function and DNA during reoxygenation to promote endothelial cell survival and reverse pulmonary hypertension. *Cell Metab* 2015;21(4):596–608; doi: 10.1016/j.cmet.2015.03.010
- Ebrahimipoor M, Spitali P, Hettne K, et al. Simultaneous enrichment analysis of all possible gene-sets: Unifying self-contained and competitive methods. *Brief Bioinform* 2020;21(4):1302–1312; doi: 10.1093/bib/bbz074
- Egnatchik RA, Brittain EL, Shah AT, et al. Dysfunctional BMPR2 signaling drives an abnormal endothelial requirement for glutamine in pulmonary arterial hypertension. *Pulm Circ* 2017;7(1):186–199; doi: 10.1086/690236
- Evans AM, DeHaven CD, Barrett T, et al. Integrated, nontargeted ultrahigh performance liquid chromatography/electrospray ionization tandem mass spectrometry platform for the identification and relative quantification of the small-molecule complement of biological systems. *Anal Chem* 2009;81(16):6656–6667; doi: 10.1021/ac901536h
- Fang YH, Piao L, Hong Z, et al. Therapeutic inhibition of fatty acid oxidation in right ventricular hypertrophy: Exploiting Randle's cycle. *J Mol Med (Berl)* 2012;90(1):31–43; doi: 10.1007/s00109-011-0804-9
- Farha S, Comhair S, Hou Y, et al. Metabolic endophenotype associated with right ventricular glucose uptake in pulmonary hypertension. *Pulm Circ* 2021;11(4):20458940211054325; doi: 10.1177/20458940211054325
- Farha S, Saygin D, Park MM, et al. Pulmonary arterial hypertension treatment with carvedilol for heart failure: A randomized controlled trial. *JCI Insight* 2017;2(16); doi: 10.1172/jci.insight.95240
- Fessel JP, Hamid R, Wittmann BM, et al. Metabolomic analysis of bone morphogenetic protein receptor type 2 mutations in human pulmonary endothelium reveals widespread metabolic reprogramming. *Pulm Circ* 2012;2(2):201–213; doi: 10.4103/2045-8932.97606
- Fijalkowska I, Xu W, Comhair SA, et al. Hypoxia inducible-factor1 α regulates the metabolic shift of pulmonary hypertensive endothelial cells. *Am J Pathol* 2010;176(3):1130–1138; doi: 10.2353/ajpath.2010.090832
- Ghosh S, Gupta M, Xu W, et al. Phosphorylation inactivation of endothelial nitric oxide synthesis in pulmonary arterial hypertension. *Am J Physiol Lung Cell Mol Physiol* 2016;310(11):L1199–L1205; doi: 10.1152/ajplung.00092.2016
- Gnaiger E. Complex II ambiguities-FADH(2) in the electron transfer system. *J Biol Chem* 2024;300(1):105470; doi: 10.1016/j.jbc.2023.105470
- Guo X, Wu J, Du J, et al. Platelets of type 2 diabetic patients are characterized by high ATP content and low mitochondrial membrane potential. *Platelets* 2009;20(8):588–593; doi: 10.3109/09537100903288422
- Hemnes AR, Leopold JA, Radeva MK, et al. PVDOMICS Study Group. Clinical characteristics and transplant-free survival across the spectrum of pulmonary vascular disease. *J Am Coll Cardiol* 2022;80(7):697–718; doi: 10.1016/j.jacc.2022.05.038
- Herve P, Humbert M, Sitbon O, et al. Pathobiology of pulmonary hypertension. The role of platelets and thrombosis. *Clin Chest Med* 2001;22(3):451–458; doi: 10.1016/s0272-5231(05)70283-5
- Humbert M, Kovacs G, Hoeper MM, et al. ESC/ERS Scientific Document Group. 2022 ESC/ERS Guidelines for the diagnosis and treatment of pulmonary hypertension. *Eur Heart J* 2022;43(38):3618–3731; doi: 10.1093/eurheartj/ehac237
- Kalhan SC, Gruca LL, Parimi PS, et al. Serine metabolism in human pregnancy. *Am J Physiol Endocrinol Metab* 2003;284(4):E733–E740; doi: 10.1152/ajpendo.00167.2002
- Kalhan SC, Guo L, Edmison J, et al. Plasma metabolomic profile in nonalcoholic fatty liver disease. *Metabolism* 2011;60(3):404–413; doi: 10.1016/j.metabol.2010.03.006

- Kaneko FT, Arroliga AC, Dweik RA, et al. Biochemical reaction products of nitric oxide as quantitative markers of primary pulmonary hypertension. *Am J Respir Crit Care Med* 1998;158(3):917–923; doi: 10.1164/ajrccm.158.3.9802066
- Kao CC, Wedes SH, Hsu JW, et al. Arginine metabolic endotypes in pulmonary arterial hypertension. *Pulm Circ* 2015; 5(1):124–134; doi: 10.1086/679720
- Klinger JR, Abman SH, Gladwin MT. Nitric oxide deficiency and endothelial dysfunction in pulmonary arterial hypertension. *Am J Respir Crit Care Med* 2013;188(6):639–646; doi: 10.1164/rccm.201304-0686PP
- Lane KL, Talati M, Austin E, et al. Oxidative injury is a common consequence of BMPR2 mutations. *Pulm Circ* 2011; 1(1):72–83; doi: 10.4103/2045-8932.78107
- Lannan KL, Phipps RP, White RJ. Thrombosis, platelets, microparticles and PAH: More than a clot. *Drug Discov Today* 2014;19(8):1230–1235; doi: 10.1016/j.drudis.2014.04.001
- Liu Q, Shepherd BE, Li C, et al. Modeling continuous response variables using ordinal regression. *Stat Med* 2017;36(27): 4316–4335; doi: 10.1002/sim.7433
- Machado RF, Londhe Nerkar MV, Dweik RA, et al. Nitric oxide and pulmonary arterial pressures in pulmonary hypertension. *Free Radic Biol Med* 2004;37(7):1010–1017; doi: 10.1016/j.freeradbiomed.2004.06.039
- Malenfant S, Potus F, Fournier F, et al. Skeletal muscle proteomic signature and metabolic impairment in pulmonary hypertension. *J Mol Med (Berl)* 2015;93(5):573–584; doi: 10.1007/s00109-014-1244-0
- McDowell RE, Aulak KS, Almoushref A, et al. Platelet glycolytic metabolism correlates with hemodynamic severity in pulmonary arterial hypertension. *Am J Physiol Lung Cell Mol Physiol* 2020;318(3):L562–L569; doi: 10.1152/ajplung.00389.2019
- Michelakis ED, Gurtu V, Webster L, et al. Inhibition of pyruvate dehydrogenase kinase improves pulmonary arterial hypertension in genetically susceptible patients. *Sci Transl Med* 2017;9(413); doi: 10.1126/scitranslmed.aao4583
- Morris CR, Kato GJ, Poljakovic M, et al. Dysregulated arginine metabolism, hemolysis-associated pulmonary hypertension, and mortality in sickle cell disease. *JAMA* 2005;294(1): 81–90; doi: 10.1001/jama.294.1.81
- Nguyen QL, Corey C, White P, et al. Platelets from pulmonary hypertension patients show increased mitochondrial reserve capacity. *JCI Insight* 2017;2(5):e91415; doi: 10.1172/jci.insight.91415
- Nguyen QL, Wang Y, Helbling N, et al. Alterations in platelet bioenergetics in Group 2 PH-HFpEF patients. *PLoS One* 2019;14(7):e0220490; doi: 10.1371/journal.pone.0220490
- Nisoli E, Carruba MO. Nitric oxide and mitochondrial biogenesis. *J Cell Sci* 2006;119(Pt 14):2855–2862; doi: 10.1242/jcs.03062
- Nozik-Grayck E, Suliman HB, Majka S, et al. Lung EC-SOD overexpression attenuates hypoxic induction of Egr-1 and chronic hypoxic pulmonary vascular remodeling. *Am J Physiol Lung Cell Mol Physiol* 2008;295(3):L422–L430; doi: 10.1152/ajplung.90293.2008
- Ozkan M, Dweik RA, Laskowski D, et al. High levels of nitric oxide in individuals with pulmonary hypertension receiving epoprostenol therapy. *Lung* 2001;179(4):233–243; doi: 10.1007/s004080000064
- Paddenberg R, Stieger P, von Lilien AL, et al. Rapamycin attenuates hypoxia-induced pulmonary vascular remodeling and right ventricular hypertrophy in mice. *Respir Res* 2007; 8(1):15; doi: 10.1186/1465-9921-8-15
- Pak O, Sommer N, Hoeres T, et al. Mitochondrial hyperpolarization in pulmonary vascular remodeling. Mitochondrial uncoupling protein deficiency as disease model. *Am J Respir Cell Mol Biol* 2013;49(3):358–367; doi: 10.1165/rmb.2012-0361OC
- Parker WD, Jr, Boyson SJ, Luder AS, et al. Evidence for a defect in NADH: Ubiquinone oxidoreductase (complex I) in Huntington's disease. *Neurology* 1990a;40(8):1231–1234; doi: 10.1212/wnl.40.8.1231
- Parker WD, Jr, Boyson SJ, Parks JK. Abnormalities of the electron transport chain in idiopathic Parkinson's disease. *Ann Neurol* 1989;26(6):719–723; doi: 10.1002/ana.410260606
- Parker WD, Jr, Filley CM, Parks JK. Cytochrome oxidase deficiency in Alzheimer's disease. *Neurology* 1990b;40(8): 1302–1303; doi: 10.1212/wnl.40.8.1302
- Piao L, Fang YH, Cadete VJ, et al. The inhibition of pyruvate dehydrogenase kinase improves impaired cardiac function and electrical remodeling in two models of right ventricular hypertrophy: Resuscitating the hibernating right ventricle. *J Mol Med (Berl)* 2010;88(1):47–60; doi: 10.1007/s00109-009-0524-6
- Piao L, Fang YH, Parikh K, et al. Cardiac glutaminolysis: A maladaptive cancer metabolism pathway in the right ventricle in pulmonary hypertension. *J Mol Med (Berl)* 2013;91(10): 1185–1197; doi: 10.1007/s00109-013-1064-7
- Rezania S, Puskarich MA, Petrusca DN, et al. Platelet hyperactivation, apoptosis and hypercoagulability in patients with acute pulmonary embolism. *Thromb Res* 2017;155:106–115; doi: 10.1016/j.thromres.2017.05.009
- Rosca MG, Hoppel CL. Mitochondria in heart failure. *Cardiovasc Res* 2010;88(1):40–50; doi: 10.1093/cvr/cvq240
- Sangiorgi S, Mochi M, Riva R, et al. Abnormal platelet mitochondrial function in patients affected by migraine with and without aura. *Cephalalgia* 1994;14(1):21–23; doi: 10.1046/j.1468-2982.1994.1401021.x
- Seyfarth HJ, Hammerschmidt S, Halank M, et al. Everolimus in patients with severe pulmonary hypertension: A safety and efficacy pilot trial. *Pulm Circ* 2013;3(3):632–638; doi: 10.1086/674311
- Sharma S, Aramburo A, Rafikov R, et al. L-carnitine preserves endothelial function in a lamb model of increased pulmonary blood flow. *Pediatr Res* 2013;74(1):39–47; doi: 10.1038/pr.2013.71
- Sharp J, Farha S, Park MM, et al. Coenzyme Q supplementation in pulmonary arterial hypertension. *Redox Biol* 2014;2: 884–891; doi: 10.1016/j.redox.2014.06.010
- Shi C, Guo K, Yew DT, et al. Effects of ageing and Alzheimer's disease on mitochondrial function of human platelets. *Exp Gerontol* 2008;43(6):589–594; doi: 10.1016/j.exger.2008.02.004
- Simonneau G, Gatzoulis MA, Adatia I, et al. Updated clinical classification of pulmonary hypertension. *J Am Coll Cardiol* 2013; 62(25 Suppl):D34–D41; doi: 10.1016/j.jacc.2013.10.029
- Simpson CE, Coursen J, Hsu S, et al. Metabolic profiling of *in vivo* right ventricular function and exercise performance in pulmonary arterial hypertension. *Am J Physiol Lung Cell Mol Physiol* 2023;324(6):L836–L848; doi: 10.1152/ajplung.00003.2023
- Smits AJ, Arkani M, In 't Veld S, et al. Distinct platelet ribonucleic acid signatures in patients with pulmonary hypertension. *Ann Am Thorac Soc* 2022;19(10):1650–1660; doi: 10.1513/AnnalsATS.202201-085OC
- Stekhoven DJ, Buhlmann P. MissForest–non-parametric missing value imputation for mixed-type data. *Bioinformatics* 2012; 28(1):112–118; doi: 10.1093/bioinformatics/btr597

- Sutendra G, Michelakis ED. The metabolic basis of pulmonary arterial hypertension. *Cell Metab* 2014;19(4):558–573; doi: 10.1016/j.cmet.2014.01.004
- Tonelli AR, Haserodt S, Aytakin M, et al. Nitric oxide deficiency in pulmonary hypertension: Pathobiology and implications for therapy. *Pulm Circ* 2013;3(1):20–30; doi: 10.4103/2045-8932.109911
- Tuder RM, Davis LA, Graham BB. Targeting energetic metabolism: A new frontier in the pathogenesis and treatment of pulmonary hypertension. *Am J Respir Crit Care Med* 2012;185(3):260–266; doi: 10.1164/rccm.201108-1536PP
- Waypa GB, Marks JD, Guzy R, et al. Hypoxia triggers subcellular compartmental redox signaling in vascular smooth muscle cells. *Circ Res* 2010;106(3):526–535; doi: 10.1161/CIRCRESAHA.109.206334
- Xu W, Cardenes N, Corey C, et al. Platelets from asthmatic individuals show less reliance on glycolysis. *PLoS One* 2015;10(7):e0132007; doi: 10.1371/journal.pone.0132007
- Xu W, Janocha AJ, Erzurum SC. Metabolism in pulmonary hypertension. *Annu Rev Physiol* 2021;83:551–576; doi: 10.1146/annurev-physiol-031620-123956
- Xu W, Kaneko FT, Zheng S, et al. Increased arginase II and decreased NO synthesis in endothelial cells of patients with pulmonary arterial hypertension. *Faseb J* 2004;18(14):1746–1748; doi: 10.1096/fj.04-2317fje
- Xu W, Koeck T, Lara AR, et al. Alterations of cellular bioenergetics in pulmonary artery endothelial cells. *Proc Natl Acad Sci U S A* 2007;104(4):1342–1347; doi: 10.1073/pnas.0605080104
- Zharikov S, Shiva S. Platelet mitochondrial function: From regulation of thrombosis to biomarker of disease. *Biochem Soc Trans* 2013;41(1):118–123; doi: 10.1042/BST20120327

Address correspondence to:

*Dr. Samar Farha
Cleveland Clinic
9500 Euclid Avenue
Cleveland, OH 44195
USA*

E-mail: farhas@ccf.org

Date of first submission to ARS Central, January 29, 2024; date of final revised submission, August 29, 2024; date of acceptance, September 21, 2024.

Abbreviations Used

6MWD	= 6-minute walk distance
ATP	= Adenosine Triphosphate
BMI	= body mass index
eGFR	= estimated glomerular filtration rate
ETC	= electron transport chain
FADH ₂	= Flavin Adenine Dinucleotide
FCCP	= carbonyl cyanide <i>p</i> -trifluoromethoxyphenylhydrazone
FCS	= Flow Cytometry Standard
FDR	= false discovery rate
FSC	= forward scatter
G	= group
GABR	= global arginine bioavailability ratio
GC/MS	= gas chromatography/mass spectrometry
HPLC	= high-performance liquid chromatography
IPTW	= Inverse Probability Treatment Weighting
LTQ	= Linear Trap Quadrupole
MAD	= median absolute deviation
MFI	= mean fluorescence intensity
mPAP	= mean pulmonary arterial pressure
NADH	= Nicotinamide Adenine Dinucleotide
NO	= nitric oxide
NT-proBNP	= N-terminal pro-brain natriuretic peptide
O ₂	= oxygen
PAH	= pulmonary arterial hypertension
PE1	= prostaglandin E1
PH	= pulmonary hypertension
PVDOMICS	= Pulmonary Vascular Disease Phenomics
RNA	= ribonucleic acid
ROS	= reactive oxygen species
rSEA	= R-package Simultaneous Enrichment Analysis
RV	= right ventricle
SD	= standard deviation
SEM	= Standard Error of the Mean
SSC	= side scatter
TCA cycle	= tricarboxylic acid cycle
TDP	= true discovery proportion
TMRE	= tetramethyl rhodamine
UHPLC/MS/MS	= ultrahigh-performance liquid chromatography/tandem mass spectrometry
WSPH	= World Symposium on Pulmonary Hypertension